



Contents lists available at ScienceDirect

Arabian Journal of Chemistry

journal homepage: www.ksu.edu.sa

Ultra-trace analysis of chromium ions ($\text{Cr}^{3+}/\text{Cr}^{6+}$) in water sample using selective fluorescence turn-off sensor with natural carbon dots mixed graphene quantum dots nanohybrid composite synthesis by pyrolysis

David Nugroho^a, Rachadaporn Benchawattananon^a, Jirapad Janshongsawang^b, Nipaporn Pimsin^b, Paweena Porrawatkul^c, Rungnapa Pimsen^c, Piyawan Nuengmatcha^d, Prawit Nueangmatcha^{c,e}, Saksit Chanthai^{b,*}

^a Department of Integrated Science, Faculty of Science, Khon Kaen University, Khon Kaen 40002, Thailand

^b Materials Chemistry Research Center, Department of Chemistry and Center of Excellence for Innovation in Chemistry, Faculty of Science, Khon Kaen University, Khon Kaen 40002, Thailand

^c Nanomaterials Chemistry Research Unit, Department of Chemistry, Faculty of Science and Technology, Nakhon Si Thammarat Rajabhat University, Nakhon Si Thammarat 80280, Thailand

^d Department of Environmental Science, Faculty of Science and Technology, Nakhon Si Thammarat Rajabhat University, Nakhon Si Thammarat 80280, Thailand

^e Department of Creative Innovation in Science and Technology, Faculty of Science and Technology, Nakhon Si Thammarat Rajabhat University, Nakhon Si Thammarat 80280, Thailand

ARTICLE INFO

Keywords:

Herbal plant extract
Graphene quantum dots (GQDs)
Carbon dots (CDs)
Biosensor
Chromium ion

ABSTRACT

This study was aimed to implement the one-pot pyrolysis for hybrid nanomaterial synthesis consisting of graphene quantum dots (GQDs) from solid citric acid and carbon dots (CDs) which was hydrothermally derived from the herbal plant extract of "*Houttuynia cordata*", denoted as Carbon Dots mixed Graphene Quantum Dots (CDs@GQDs). The nanohybrid were structurally characterized by XPS, FT-IR, Fluorescence, and UV-Visible absorption spectroscopy, and their morphological images were also analyzed by HR-TEM and FE-SEM/EDX. The quantum yield was found to be 15 %, higher than that of intact CDs or GQDs. Upon excitation at a maximum wavelength of 355 nm, and emission in the 450 nm. In this case, it was observed that the nanohybrid exhibit a high degree of selectivity towards Cr^{6+} ion when employed as a fluorescence quenching sensor from screening test with different metal ions. Therefore, the optimization conditions of solution pH, concentration of nanohybrid, H_2O_2 concentration as an oxidizing agent, reaction duration time with the aid of ultrasonication were carried out in details and the permissible limit of Cr^{3+} presence in the target analyte was all undertaken in order to enhance the detection of Cr^{6+} species. Its linear calibration curve was such $y = 0.37x + 55.7$, with a coefficient of determination (r^2) value of 0.9816. The limit of detection (LOD) and limit of quantification (LOQ) was found to be 17.2 nM, and 52.2 nM. Consequently, the nanohybrid as a green chelating agent in the selective assessment of ultra-trace amount of Cr^{6+} in spiked water sample model was also done with good recoveries in both bottled drinking water and tap water samples ranging from 102.86 to 114.23 %.

1. Introduction

High quantities of heavy metals are commonly detected as water contaminants, particularly in groundwater located in areas that have been impacted by industrial activities. The source of toxicity lies in the fact that heavy metals not only contaminate drinking water, but also the soil, leading to their accumulation in plants and animals. This

accumulation poses substantial health risks to human beings. Since heavy metal pollution has a negative effect on the ecology, agricultural productivity, and human health, it has become a major worry in recent years (Tariq et al., 2021). Chromium ions are also heavy metals that can enter into soil and water sources through wastewater and solid waste as a result of its use in metallurgy, electroplating, metal processing, and other industrial industries. The stable states of Cr^{3+} and Cr^{6+} are what

Peer review under responsibility of King Saud University. Production and hosting by Elsevier.

* Corresponding author.

E-mail address: sakcha2@kku.ac.th (S. Chanthai).

<https://doi.org/10.1016/j.arabjc.2023.105443>

Received 2 October 2023; Accepted 5 November 2023

Available online 7 November 2023

1878-5352/© 2023 The Authors. Published by Elsevier B.V. on behalf of King Saud University. This is an open access article under the CC BY-NC-ND license (<http://creativecommons.org/licenses/by-nc-nd/4.0/>).

exist when Cr is introduced to the environment. Cr^{3+} being slightly less toxic than Cr^{6+} , it can still have negative health effects, especially on the skin and lungs. When compared to Cr^{3+} , Cr^{6+} has higher levels of toxicity, carcinogenicity, and mutagenicity (Sokoll et al., 2015; Shobana et al., 2017; Kart et al., 2016; Chen et al., 2019; Itzleuov et al., 2020). The hazardous metal hexavalent chromium (Cr^{6+}) especially can cause lung cancer in the human, is well-known (Anderson et al., 1983; Machle and Gregorius, 1948; Rahman et al., 2020; Dayan and Paine, 2001; Chaabane et al., 2017; Suchana et al., 2020). Therefore, the assessment of chromium characteristics holds significant significance in the prompt detection and diagnosis of these problems. Currently, various analytical methods have been utilized in the determination of Cr^{3+} and Cr^{6+} ions, such as high-performance liquid chromatography (HPLC) (Almaguer-Busso et al., 2009), solid phase extraction (Vassileva et al., 2000), inductively coupled plasma mass spectrometry (ICP-MS) (Cieslak et al., 2013; Onchoke and Sasu, 2016), voltammetry (Abbasi and Bahiraei, 2012), capillary electrophoresis (Himeno et al., 1998), RP-HPLC (Hos-sain et al., 2005), and flame atomic absorption spectrometry (FAAS) (Zhan et al., 2019). Despite the high sensitivity and selectivity of these techniques, they necessitate laborious sample preparation and pre-concentration procedures, costly instrumentation, and trained people. The challenge of developing straightforward analytical methods for the detection of Cr^{3+} and Cr^{6+} ions in natural samples persists. The utilization of light-emitting quantum-sized grapheme quantum dots (GQDs) and carbon dots (CDs) has recently garnered significant interest as a potential alternative in various industries (Guo et al., 2013; Posthuma-Trumpie et al., 2012; Wang et al., 2018; Gontrani et al., 2022; Manjunatha et al., 2023; Manjunatha et al., 2021). The utilization of GQDs and CDs in chemical sensing for the purpose of detecting metal ions is highly attractive due to their advantageous characteristics, including facile synthesis, elevated quantum yield, enhanced sensitivity and selectivity, compatibility with biological systems, adjustable emission properties, cost-effectiveness, excellent photostability, and absence of toxicity (Wang et al., 2011; Nugroho et al., 2022; Tao et al., 2012; Gao et al., 2016; Morozan and Jaouen, 2012). Furthermore, GQDs and CDs exhibit exceptional optical, electrical, and thermal characteristics, in addition to the aforementioned properties. Combining sensors with the capability to detect harmful metal ions is widely regarded as a highly favored approach (Nugroho et al., 2022; Lim et al., 2015; Varun et al., 2018). Due to this rationale, it is imperative for GQDs and CDs to enhance their surface properties in order to achieve high selectivity, excellent sensitivity, differential sensitivity for limit of detection, user-friendly sensor operation, and robust stability (Lei et al., 2021; Tetsuka et al., 2016; Haider et al., 2016). *Houttuynia Cordata* has been a subject of interest for individuals across various cultures since antiquity. *Houttuynia cordata*, commonly known as *Houttuynia cordata*, a colorful nature, is a rhizomatous, herbaceous, and perennial plant that is

indigenous to regions such as China, Japan, Korea, and Southwest Asia (Tetsuka et al., 2016). Typically, it exhibits growth patterns in areas characterized by shade and high levels of moisture (Lu et al., 2006). Historically, *Houttuynia cordata* has been utilized for medicinal purposes by individuals. A substantial body of scientific evidence supports the notion that *Houttuynia cordata*, whether in its entirety or in the form of derived extracts, has noteworthy therapeutic properties. *Houttuynia cordata* possesses a diverse array of chemical compounds that exhibit distinct therapeutic effects and can be classified into many chemical classes, including alkaloids, essential oils, and flavonoids (Park et al., 2005; Chiang et al., 2003; Chang et al., 2001; Li et al., 2017; Ma et al., 2017; Chou et al., 2009; Ahn et al., 2017).

This study introduces a newly designed fluorescence sensor probe and presents a method for the specific detection of Cr^{6+} in drinking water samples (see graphical abstract in Fig. 1). The synthesis of sensor probe CDs@GQDs hybrid composite involves the combination of carbon dots derived from the *Houttuynia cordata* extract with GQDs obtained from citric acid using a straightforward, environmentally friendly, and economically viable one-pot pyrolysis process. Nevertheless, there is a scarcity of documented findings regarding the utilization of CDs with GQDs for Cr^{6+} detection. The optical characteristics of CDs@GQDs exhibit remarkable selectivity and stability in detecting Cr^{6+} . This study extensively examined the impact of solution pH, masking agents, and interfering ions. Subsequently, the established technique was employed to ascertain the concentration of hexavalent chromium (Cr^{6+}) ions in authentic water samples.

2. Materials and methods

2.1. Materials and reagents

All compounds utilized in this study were of analytical grade. The citric acid anhydrous (99.5 %) and sodium hydroxide micropearls (99 %) used in this study were sourced from Carlo Erba, an Italian manufacturer. 50 % hydrogen peroxide was acquired from Paramount Chemical, an Australian supplier. The ethylenediaminetetraacetic acid (99.4 – 100.06 %) was procured from Sigma-Aldrich, a reputable supplier based in Germany. The procurement of paraffin oil liquid with density 25/25 was conducted through the acquisition from Ajex Finechem, an Australian supplier. The trials were conducted using deionized water obtained from the Simplicity Water Purification System, Model Simplicity 185, manufactured by Millipore in the United States.

2.2. Instruments and apparatus

The primary instrument employed for this study was a Shimadzu RF-5301PC Spectrofluorophotometer. The UV-visible spectrophotometer

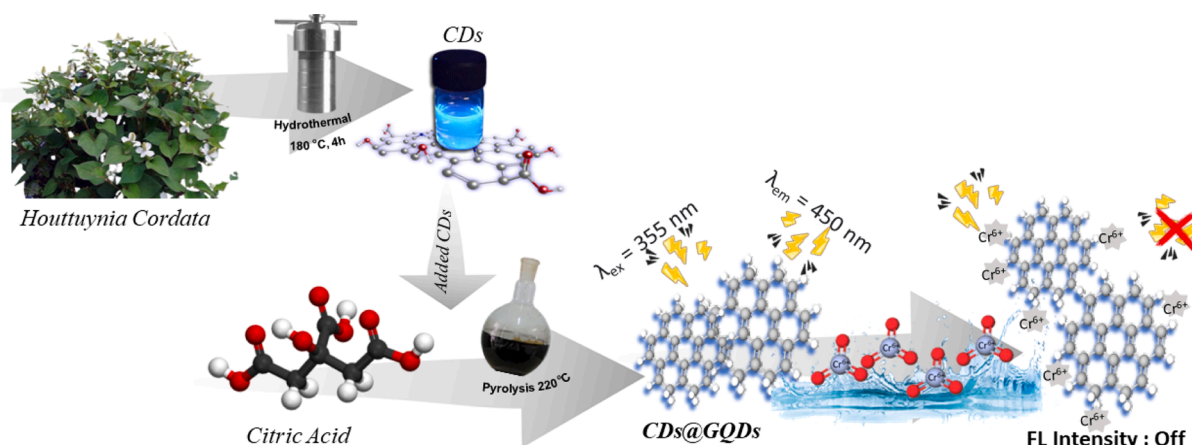


Fig. 1. The graphical abstract of the as-synthetic CDs@GQDs hybrid composite for Cr^{6+} detection.

utilized in this study was the Agilent 8453 model. The following instruments were utilized in the experiment: the pH meter UB-10 Ultra-Basic, the analytical balance Model LX 220A, the quartz cell with a path length of 1 cm obtained from Fisher Scientific, and the Ultrasonic Cleaner Model VGT-2300. A measurement using attenuated total reflectance-Fourier transform infrared ATR-FTIR spectroscopy was conducted using a TENSOR27 system Fourier transform infrared spectrometer. The study employed transmission electron microscopy TEM with a Schottky field emission type electron gun. The EDX spectra were acquired using HITACHI S-3000 N scanning electron microscope (SEM). The citric acid pyrolysis experiment was conducted using a round bottom flask manufactured by Pyrex®. A heated plate equipped with a magnetic stirrer was used in conjunction with a paraffin oil bath. The CHNS method by using ThermoScientific Flash 2000 N/Protein analyzer.

2.3. Preparation of carbon dots (CDs) and graphene carbon dots (GQDs)

The preparation of carbon dots (CDs) involved the addition of 20 mL of *Houttuynia cordata* aqueous extract into a teflon cup for hydrothermal synthesis. The tank was then placed in an oven set at a temperature of 180 °C for a duration of 4 h. Following the completion of the synthesis process, centrifugation was carried out at a speed of 10000 rpm for a period of 10 min.

Graphene carbon dots (GQDs) has been prepared by one-pot synthesis pyrolysis method using 1 g citric acid into a 100 mL round bottom flask. The flask was then subjected to heating within the temperature range of 220–240 °C, utilizing a paraffin oil bath for a duration of around 5 min. Subsequently, the liquid combination was dissolved with the gradual addition of 50 mL of 0.25 M NaOH solution, with continuous agitation for a duration of 30 min.

2.4. Preparation of CDs@GQDs hybrid composite

5 mL of CDs and 1 g of citric acid add into a 100 mL round bottom flask. The flask was then subjected to heating within the temperature range of 220–240 °C, utilizing a paraffin oil bath for a duration of around 5 min. Subsequently, the liquid combination was dissolved with the gradual addition of 50 mL of a 0.25 M NaOH solution, with continuous agitation for a duration of 30 min. The resultant hybrid nature of both CDs and GQDs, noted as “CDs@GQDs”, was kept cool in refrigerator (4 °C) until further use.

2.5. Screening test of various metal ions using fluorescence quenching effect

The fluorescence analysis using the CDs@GQDs was conducted with a Britton – Robinson buffer solution pH 12.2. In the subsequent trials, a solution of CDs@GQDs with a concentration of approximately 100 mgL⁻¹ was thoroughly mixed in a 10 mL volumetric flask. Subsequently, different quantities ranging from nM to mM of Mⁿ⁺ were introduced into a portion of the CDs@GQDs solution, resulting in a final volume of 10 mL at ambient temperature. Various metal ions (Cr³⁺, Zn, Mg, Fe²⁺, Cr⁶⁺, Ni, Co, Fe³⁺, Mn, Cd, Pb) were applied under this experimental condition in the same manner. The fluorescence quenching sensor of each solution including CDs@GQDs was measured promptly at the excitation/emission maximum wavelengths of $\lambda_{ex}/\lambda_{em} = 355/460$ nm.

2.6. Optimization study for chromium ions selectivity

The selective optimization for chromium (VI) detection was studied in this research including a variety of tests, such as reaction time, temperature, the effect of interfering ions on Cr⁶⁺ using different NaCl concentrations, the effect of pH solutions, and the effect of EDTA concentration. The oxidation effect of Cr³⁺ → Cr⁶⁺ with hydrogen peroxide (H₂O₂) was also studied in such case having the Cr³⁺ species being presence in the sample.

2.7. Method validation

Evaluation of an analytical method is consistently assessed based on its appropriateness for the intended purpose, recovery capability, need for standardization, sensitivity, stability of the analyte, ease of analysis, necessary skill set, as well as time and cost considerations, in that particular sequence. It is of utmost importance to rigorously ascertain, via a systematic procedure, the suitability of the analytical method in question for its intended objective. The determination of the limit of detection (LOD), limit of quantitation (LOQ), and percentage recovery (% Recovery) are critical parameters in the process of method validation within the field of analytical chemistry. Both LOD and LOQ are utilized to characterize the minimum concentration of an analyte that can be accurately determined by an analytical method. On the other hand, the percentage recovery is employed to ascertain the proportion of the original material that is obtained following the completion of a chemical reaction. In this study, the determination of LOD is performed using the formula $LOD = 3SD/S$, while LOQ is calculated using the formula $LOQ = 10SD/S$. In these calculations, SD denotes the standard deviation of the blank readings multiplied by three, and S indicates the slope of the linear regression plot. The calculation of recovery is performed using the formula $\% \text{ recovery} = C_{\text{found}} / C_{\text{added}} \times 100$. In this context, C_{found} denotes the concentration of the analyte subsequent to the introduction of a known quantity of standard into the actual sample. C_{added} signifies the concentration of the analyte inside the actual sample, while C_{added} reflects the concentration of the known quantity of standard that was spiked into the real sample (Pimsin et al., 2022; Nugroho et al., 2023).

2.8. Applicable detection of Cr⁶⁺ in spiked water sample

In order to evaluate the effectiveness of a fluorescence sensor utilizing CDs@GQDs for the Cr⁶⁺ detection in an artificial system, the suitability of this developed method for analyzing real water samples, such as tap water and drinking water, was investigated. Drinking water were purchase from market in Khon Kaen university, and untreated tap water samples were obtained from the Khon Kaen district and stored in polyethylene bottles. In this experimental protocol, a volume of 1 mL of the water sample was combined with 1 mL of a solution containing CDs@GQDs at a concentration of 100 mgL⁻¹. The resulting mixture was then placed into a 10.0 mL volumetric flask. Subsequently, the individual sample mixture was spiked with different concentrations of Cr⁶⁺ standard solution (25, 50 & 75 nM) in a manner consistent with the recovery study, prior to conducting the fluorescence measurements.

3. Results and discussion

3.1. Characterization of the as-synthesized CDs@GQDs hybrid composite

3.1.1. FT-IR and XPS spectroscopy

The CDs@GQDs synthesized using a one-pot pyrolysis method were subjected to analysis of functional groups, elemental atoms, and chemical bonds using Fourier transform infrared spectrometry (FTIR) and X-ray photoelectron spectroscopy (XPS). The FTIR spectral analysis, as depicted in Fig. 2a, provides confirmation of the presence of specific peaks at approximately 3300 cm⁻¹, which can be attributed to the vibrations of O–H (Chou et al., 2009). Additionally, the peak observed at 2930 cm⁻¹ indicates the presence of methyl, methylene, and aromatic hydrogens within the chemical structure of the sample (Chou et al., 2009). The peak at 2345 cm⁻¹ is consistent with the typical asymmetric stretching of adsorbed CO₂ (Ahn et al., 2017). Furthermore, the peak observed at 1000 cm⁻¹ is assigned to C–O bonds. These findings provide evidence that the CDs@GQDs hybrid are the nanoparticle product obtained from a fine coupling of GQDs derived from the pyrolysis of citric acid in the presence of the hydrothermally derived CDs from the herbal extract.

X-ray photoelectron spectroscopy (XPS) was utilized to ascertain the

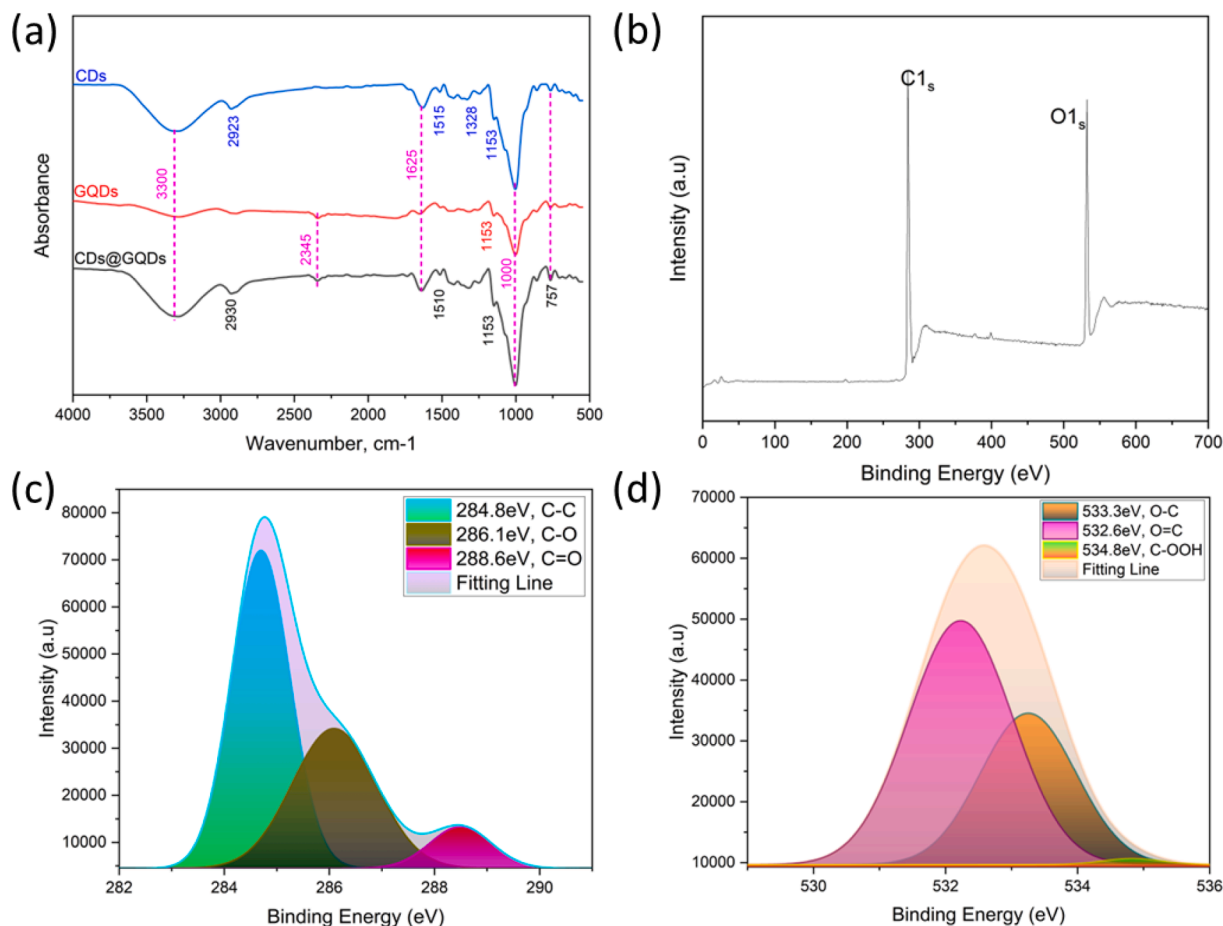


Fig. 2. Spectroscopy characteristics of CDs@GQDs by (a) FTIR (b) XPS-Survey data of CDs@GQDs, and high resolution XPS spectra of (c) C1s and (d) O1s.

elemental compositions, carbon bonding, and oxygen bonding within the as-synthesized CDs@GQDs. Fig. 2b displays the survey spectrum of the CDs@GQDs. The observed peaks at approximately 284.04 and 532.08 eV may be attributed to the binding energy of carbon (C1s) and oxygen (O1s), respectively. In the case of C1s (Fig. 2c), the XPS analysis reveals the existence of C–C, C–O, and C = O functional groups. (Aumber et al., 2020) The deconvoluted binding energies corresponding to these groups are seen at 284.8, 286.1, and 288.6 eV, respectively. As depicted in Fig. 2d, the high-resolution XPS spectra of CDs@GQDs revealed a significant presence of oxygen functional groups. This observation suggests that the carbonization process of CDs@GQDs during pyrolysis was incomplete. Furthermore, the O1s spectra of CDs@GQDs exhibited three supplementary peaks at 533.3, 532.6, and 534.8 eV, which can be attributed to the O–C, O = C, and C–OOH bonds, respectively. (Aumber et al., 2020) The composition of the CDs@GQDs material consists of 57.91 % carbon and 42.09 % oxygen, as determined through the analysis of XPS spectra. Table 1 presents the elemental composition percentages of CDs, GQDs, and CDs@GQDs, as determined using CHNS analysis. The results indicate that the CDs@GQDs exhibit a carbon content of 60.31 % and a hydrogen one of 9.72 %.

Table 1
C - H composition analysis of CDs, GQDs and CDs@GQDs samples.

Sample	C%	±SD, n = 3	H%	±SD, n = 3
CDs	53.46	1.06	11.87	1.45
GQDs	63.77	1.95	9.02	1.40
CDs@GQDs	60.31	1.41	9.72	1.17

3.1.2. HR-TEM and FE-SEM/EDX image analysis

The utilization of a field emission scanning electron microscope (FE-SEM) allows for the observation of a surface morphology with high resolution. This enables the examination of the surface texture variations of the manufactured carbon dots (CDs), graphene quantum dots (GQDs), and the hybrid CDs@GQDs. Furthermore, the FE-SEM analysis provides valuable insights into the distribution of elements within these materials. Fig. 3a displays a representative SEM picture of carbon dots (CDs). The CDs have a smooth, level surface and display a spherical appearance. Additionally, they possess the property of easily melting at room temperature. Fig. 3b illustrates the presence of broad ridges and a rough, yet regular, surface structure in GQDs. The successful functionalization of CDs and GQDs is demonstrated by the surface of CDs@GQDs, as depicted in Fig. 3c. The elemental compositions of CDs, GQDs, and CDs@GQDs are also verified by the energy-dispersive X-ray spectroscopy (EDX) as shown in Fig. 3d, e, and f, respectively. The CDs were discovered to have compositional constituents consisting of 76.7 % carbon (C) and 22.6 % oxygen (O), as depicted in Fig. 3d. The GQDs exhibited a compositional element consisting of 54.1 % carbon (C) and 44.2 % oxygen (O) (Fig. 3e). The compositional constituents of the CDs@GQDs were determined to be 64.2 % carbon (C) and 33.8 % oxygen (O) (Fig. 3f). It was reliable that the *in situ* GQDs produced in the presence of the CDs would attribute to disrupt their structural environment of the hybrid nanoparticles. In addition, transmission electron microscopy (TEM) examination was conducted to examine the structural and morphological characteristics of the hybrid samples, demonstrating homogeneous layer texture. The particle size of the CDs@GQDs is observed to be around ± 2.7 nm as shown in Fig. 3g.

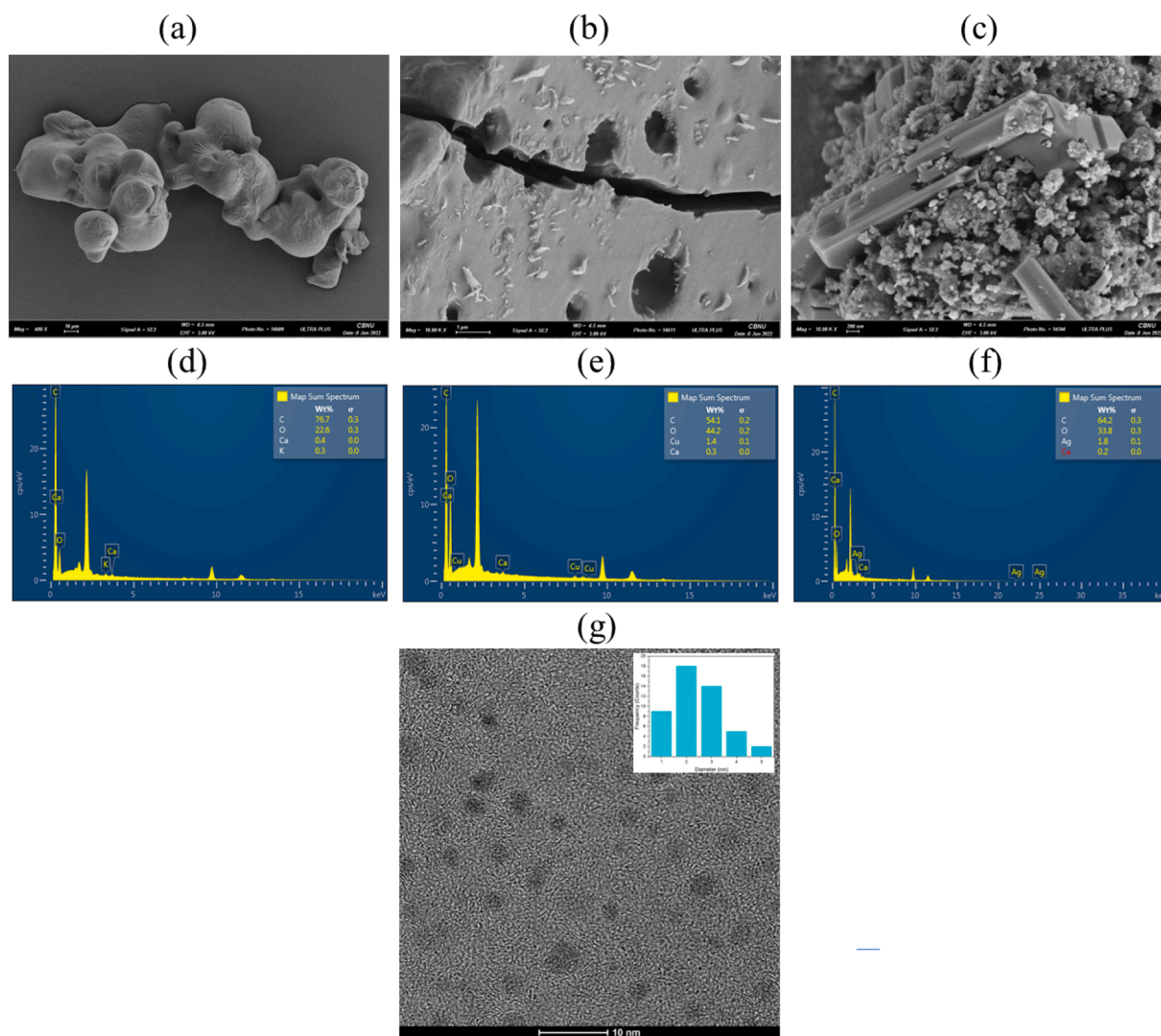


Fig. 3. FE-SEM images of (a) CDs (b) GQDs & (c) CDs@GQDs, and EDX of (d) CDs (e) GQDs & (f) CDs@GQDs, and (g) TEM image of CDs@GQDs.

3.2. Optical properties of the CDs@GQDs

3.2.1. Fluorescence property and relative quantum yield

Fig. 4 depicts the fluorescence spectra of the carbon dots (CDs), graphene quantum dots (GQDs), and the hybrid composite CDs@GQDs. The CDs exhibit emission and excitation maximum wavelengths at 340 and 438 nm, respectively, with an intensity of 300 relative arbitrary unit. On the other hand, GQDs exhibit emission and excitation maximum wavelengths at 360 and 460 nm, respectively, with an intensity of 440 rel. arb. unit. Upon the CDs doped into GQDs, resulted the nanohybrid composite CDs@GQDs, the intensity significantly increases up to 980 rel. arb. unit with their emission and excitation wavelengths of 355 and 450 nm, respectively under the same slit width of the instrument. The quantum yields (Q) of CDs, GQDs, and CDs@GQDs were determined through a comparative analysis of their integrated fluorescence intensities and absorbance values in relation to quinine sulfate. The $Q = 0.54$ of the quinine standard solution, when dissolved in a 0.1 M H_2SO_4 solution, is used as reference. Table 2 presents a compilation of the quantum yields associated with various doping materials. The fluorescence quantum yields (FQ) of the synthesized CDs, GQDs, and the hybrid CDs@GQDs were determined to be 8 %, 13 % and 15 %, respectively. The FQ of CDs, GQDs and CDs@GQDs was calculated with the following equation from a|e - UV-Vis-IR Spectral Software (Fletcher, 1969; Pimsin et al., 2022). From diffused reflectance spectra, the

calculation of band gap energy using Tauc Plot of CDs, GQDs and CDs@GQDs were done as shown in Fig. 4c and Fig. 4d, their band gap energy of CDs@GQDs (5.06 eV) is quite wider than those of CDs (4.94 eV) and GQDs (4.90 eV).

3.3. Fluorescence quenching effect of Cr^{6+} using CDs, GQDs and CDs@GQDs

The selectivity test of the CDs for various metal ions (Cr^{3+} , Zn, Mg, Fe^{2+} , Cr^{6+} , Ni, Co, Fe^{3+} , Mn, Cd, Pb) is shown in the Fig. 5a. The CDs from *Houttuynia cordata* extract gave its selectivity with Fe^{2+} . Fe^{2+} exhibits strong affinity towards of CDs, and it becomes high potential selectivity with the CDs. Fig. 5b shows the results of the metal ions detection experiments using GQDs, indicating that the GQDs have the quenching effect of Fe^{2+} and Cr^{6+} with having their intensity that are not significantly distinct. After CDs doped with the GQDs the selectivity for detection heavy metal ion was selective to detect hexavalent chromium (Cr^{6+}) only as clearly shown in Fig. 5c. The quenching effect of CDs@GQDs as determined by $F_0 - F$, where F_0 and F are the fluorescent intensities of blank and with different concentrations of the metal ions shown in the Fig. 5d, respectively. The experiments were involved doing fluorescence quenching tests using different heavy metal ions (0.5 M). It was observed that the presence of Cr^{6+} ions resulted in a significant reduction of around 89 % in the fluorescence emission of the carbon

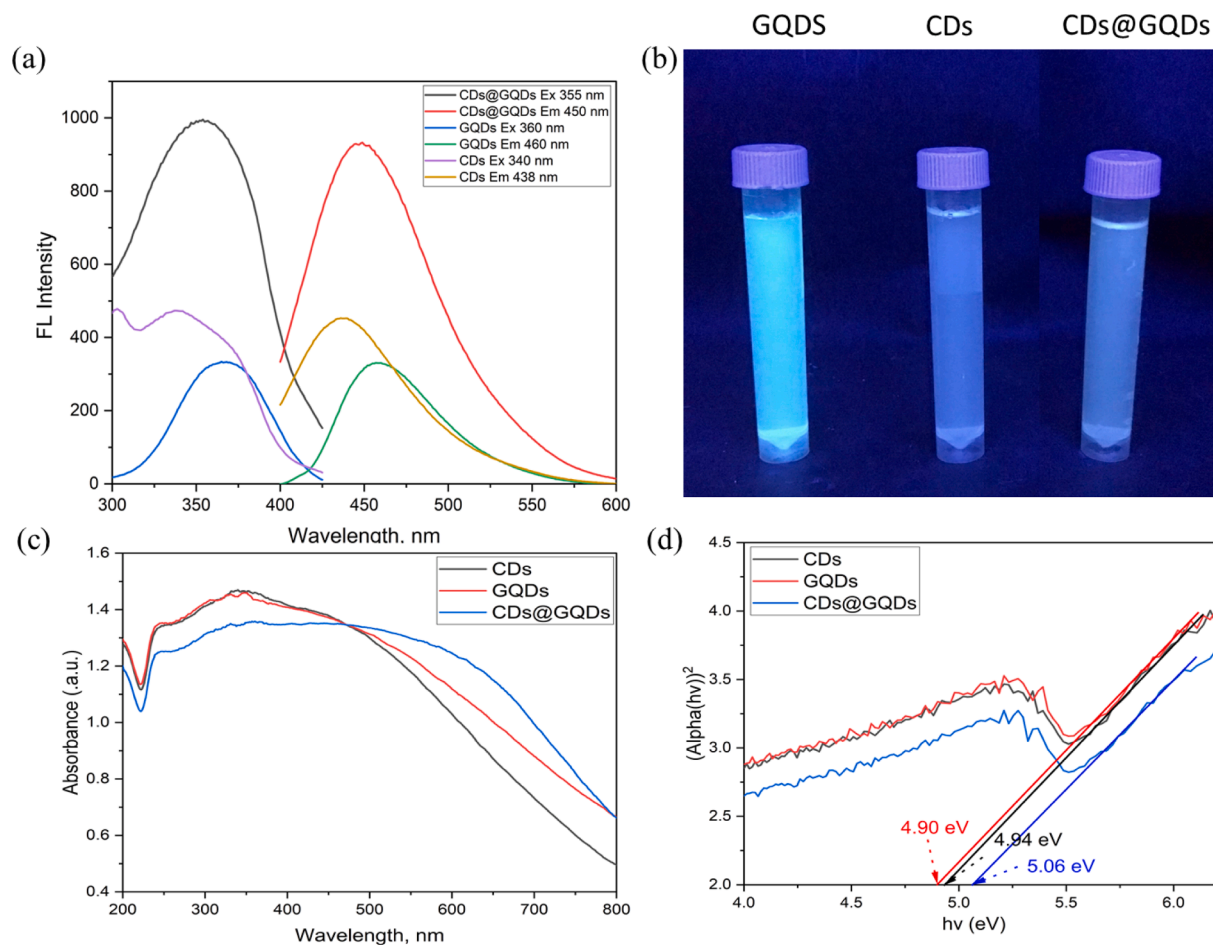


Fig. 4. The Fluorescence spectra of CDs, GQDs and CDs@GQDs under the optimum conditions, (b) comparison of the instinct blue solution of CDs, GQDs and CDs@GQDs under commercial UV light. (For interpretation of the references to colour in this figure legend, the reader is referred to the web version of this article.)

Table 2
Quantum yields of the CDs, GQDs and CDs@GQDs samples.

Material	Quantum yield (%)
CDs	8
GQDs	13
CDs@GQDs	15

dots. The significant and specific suppression of fluorescence exhibited by Cr^{6+} ions can be attributed to the formation of hydrogen bonds between Cr^{6+} and carbon dots. This interaction inhibits the release of fluorescence emissions, which results in a low intensity of fluorescence (Bu et al., 2016; Onchoke and Sasu, 2016).

3.4. Effect of EDTA as general masking agent for heavy metals

In order to investigate the efficacy of EDTA as a broad-spectrum masking agent for the detection of heavy metal ions in an aqueous sample, various concentrations of EDTA (0.01, 0.1, 0.25, 0.5 and 1 M) were added into a solution containing 100 μL of CDs@GQDs. Additionally, 10 μL of Cr^{6+} ion with a concentration of 0.5 M were included in the solution. The resulting mixture was then adjusted to a final volume of 10 mL in a volumetric flask, after which fluorescence measurements were conducted. The obtained fluorescence spectra were subsequently recorded and depicted in Fig. 6. The addition of EDTA did not exhibit any significant alterations or any discernible impact on the reaction between Cr^{6+} and the CDs@GQDs.

3.5. Effect of solution pH

The effect of the solution pH towards the fluorescence quenching of CDs@GQDs was also studied by adding various pH values into 0.5 M of Cr^{6+} . According to the results on Fig. 7, the solution pH ranges of 3 to 13 gave a significant effect for Cr^{6+} detection with the optimal condition pH 12. Therefore, the solution pH 12 was preferred for further study in this study.

3.6. Effect of H_2O_2 in the oxidation of Cr^{3+} to become Cr^{6+} expressed as total amount of Cr

The effect of Cr^{3+} on the determination of Cr^{6+} in the sample solution by this proposed fluorescence quenching sensor was studied. Three concentration ranges (0.5 μM , 0.5 mM & 0.5 M) of each Cr^{3+} and Cr^{6+} were prepared and mixed with CDs@GQDs as shown in Fig. 8a. It was found that Cr^{3+} mixed with Cr^{6+} did not show any effect for selectivity test. The oxidation effect of Cr^{3+} was studied by using various concentrations of H_2O_2 . Fig. 8b shows when increasing the concentration of H_2O_2 with 0.5 M Cr^{3+} , the optimum condition of H_2O_2 was about 15%.

3.7. Effect of reaction time and temperature of CDs@GQDs with Cr^{6+}

The reaction between CDs@GQDs and 0.5 nM Cr^{6+} at different time intervals and temperatures was carried out. The results are presented in Fig. 9a. When CDs@GQDs were combined with Cr^{6+} under two different conditions, one involving sonication and the other without sonication, it was observed that the reaction time from 1 min until 15 min did not

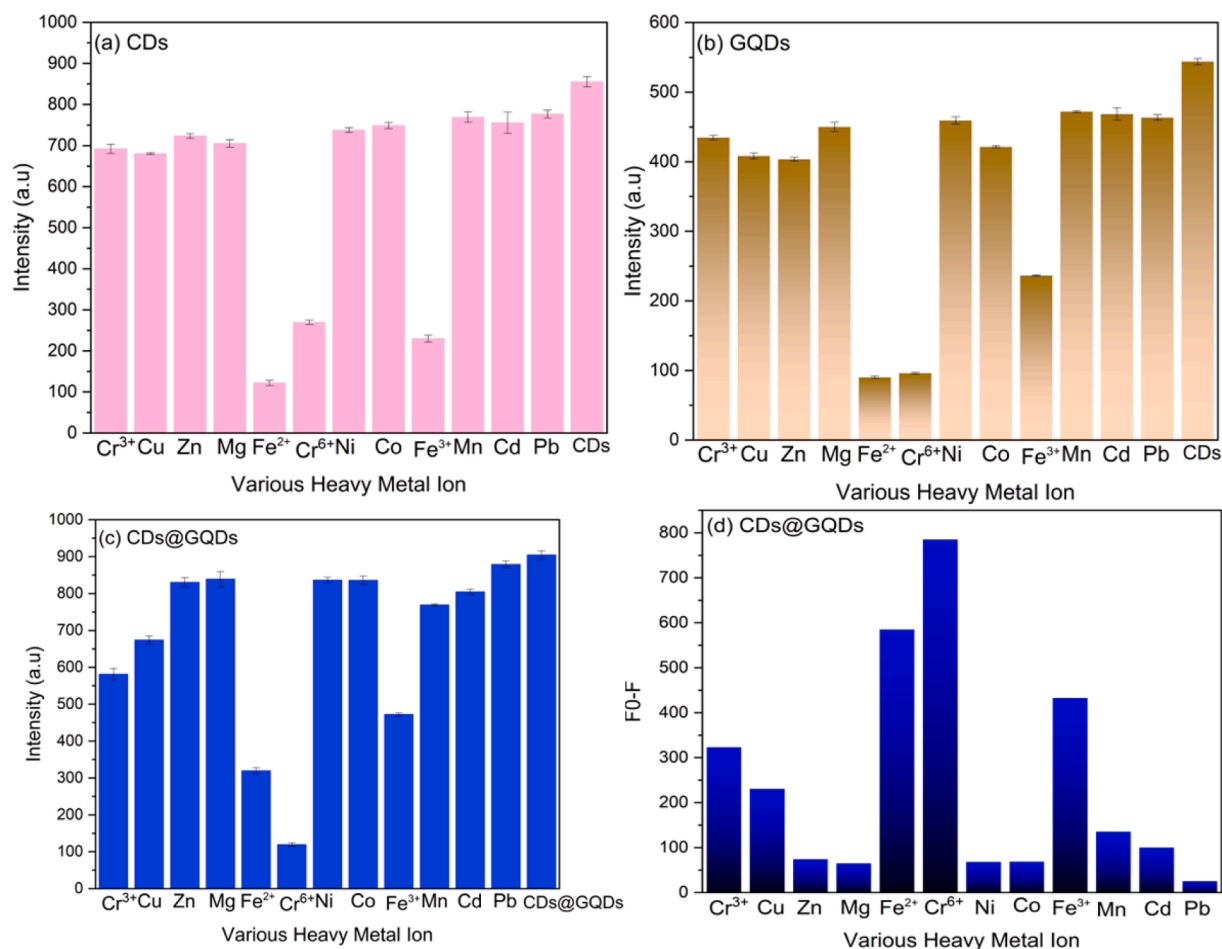


Fig. 5. Comparison of the fluorescent intensities of various metal ions by using (a) CDs, (b) GQDs and (c) CDs@GQDs ($n = 3$), and (d) $F_0 - F$ of CDs@GQDs represents the quenching effect of heavy metal ions.

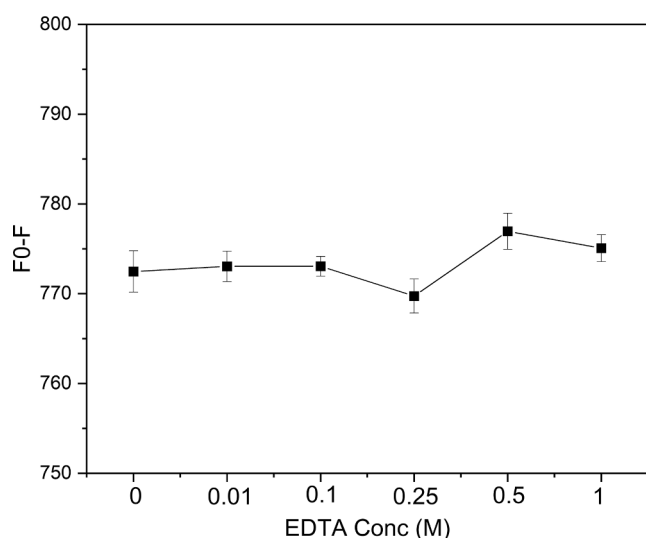


Fig. 6. Effect of EDTA concentrations for Cr⁶⁺ detection.

affect the desired intensity in two of condition. However, the temperature reaction of CDs@GQDs and Cr⁶⁺ had a significant impact on the fluorescence reaction especially at 45 °C the $F_0 - F$ show higher than other conditions as shown in Fig. 9b.

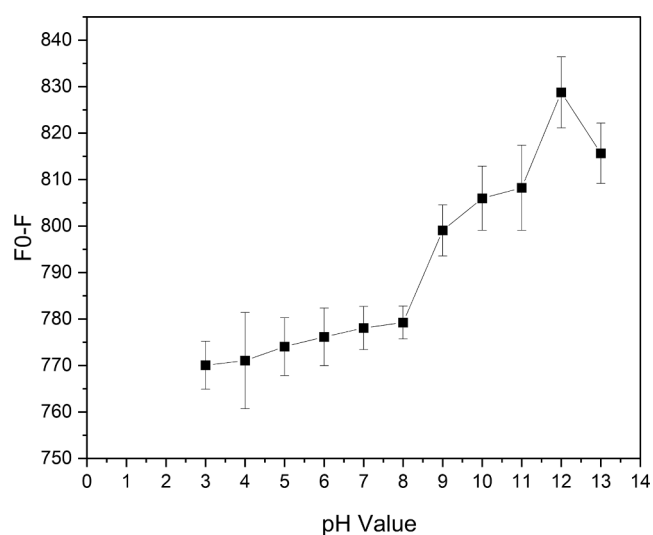


Fig. 7. Effect of the solution pH on Cr⁶⁺ detection.

3.8. Effect of an ionic strength

The effect of sodium chloride (NaCl) as an ionic strength on the interactions between Cr⁶⁺ and the CDs@GQDs nanohybrid composite has been studied, various condition of NaCl has been applied (0.1, 0.5, 1, 2.5 and 5 M). Fig. 10 depicts the influence of a 5 M NaCl solution on the

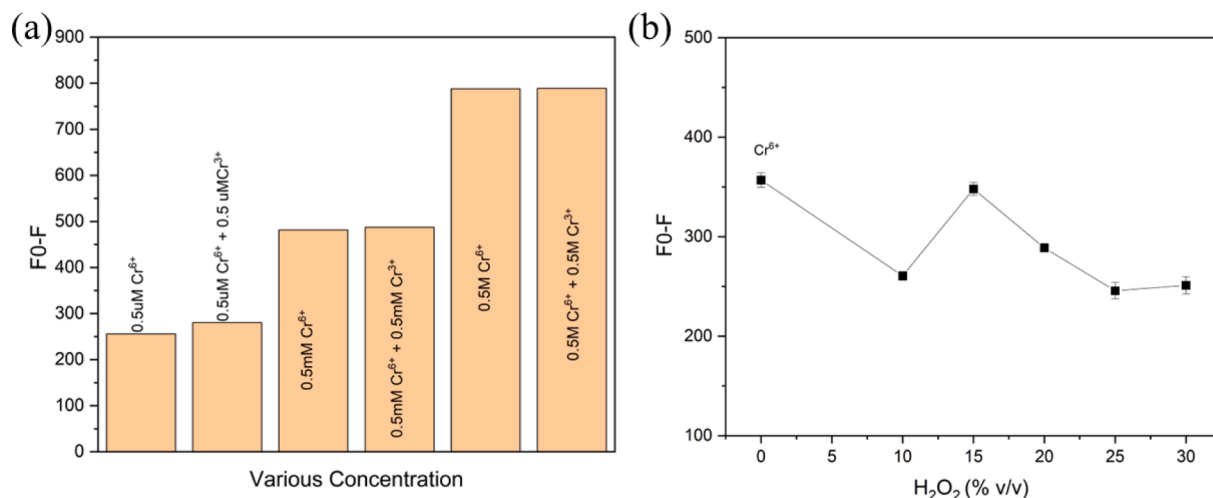


Fig. 8. (a) Comparison of three concentration ranges of Cr³⁺ (0.5 uM, 0.5 mM & 0.5 M) and Cr⁶⁺ (0.5 uM, 0.5 mM & 0.5 M) via the fluorescence quenching effect of Cr³⁺ (b) Oxidation effect of H₂O₂ concentrations on Cr³⁺ vs Cr⁶⁺ (without H₂O₂) as reference.

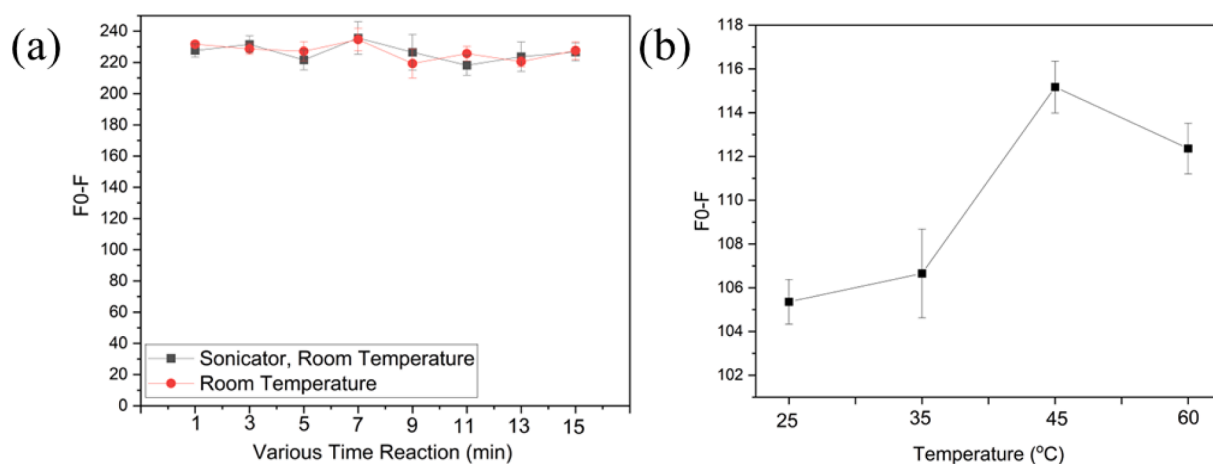


Fig. 9. (a) Effects of various time duration reaction between normal condition and under sonicator at room temperature, and (b) the effect of heating temperature on the fluorescence quenching effect of Cr⁶⁺.

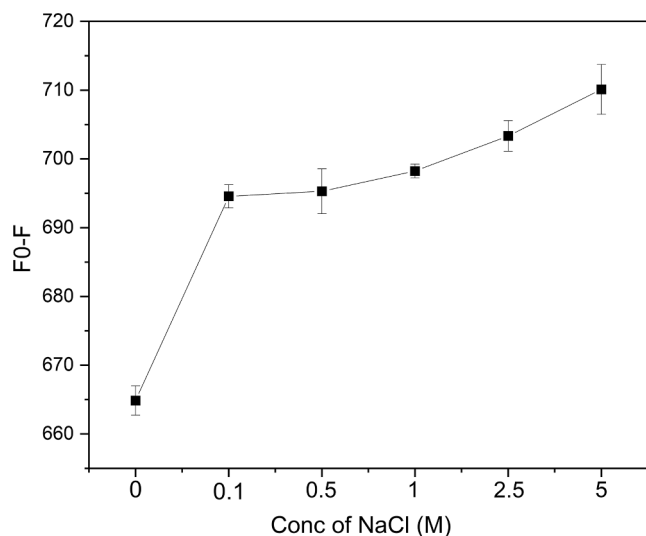


Fig. 10. Effect of ionic strength using various concentrations of NaCl on the fluorescence quenching effect of Cr⁶⁺.

detection of Cr⁶⁺, somewhat leading to enhanced selectivity of the fluorescence quenching system.

3.9. The analytical characteristics of the developed fluorescence sensing probe

With the aim to examine the effectiveness of the fluorescence quenching sensor in the target detecting of Cr⁶⁺, the developed methodology was subjected to a validation process for quantitative purposes. This validation method includes the evaluations of linearity, detection limit (LOD), quantification limit (LOQ), accuracy (as % recovery) and precision (as % reproducibility).

3.9.1. Linearity

A study on linearity was conducted to examine the impact of varying concentrations of Cr⁶⁺ on the fluorescence intensity of CDs@GQDs. Fig. 11 illustrates the fluorescence spectra of the CDs@GQDs at varying doses of Cr⁶⁺ and Cr³⁺ plus H₂O₂. The spectral analysis reveals that the fluorescence intensity of the CDs@GQDs exhibit a high degree of sensitivity in response to variation in the Cr⁶⁺ concentration. The fluorescence intensity exhibits a decrease as the concentration of Cr⁶⁺ increases. Therefore, the determination of the quenching efficiency of Cr⁶⁺ was conducted using the linear equation ($F_0 - F$), where F_0 represents

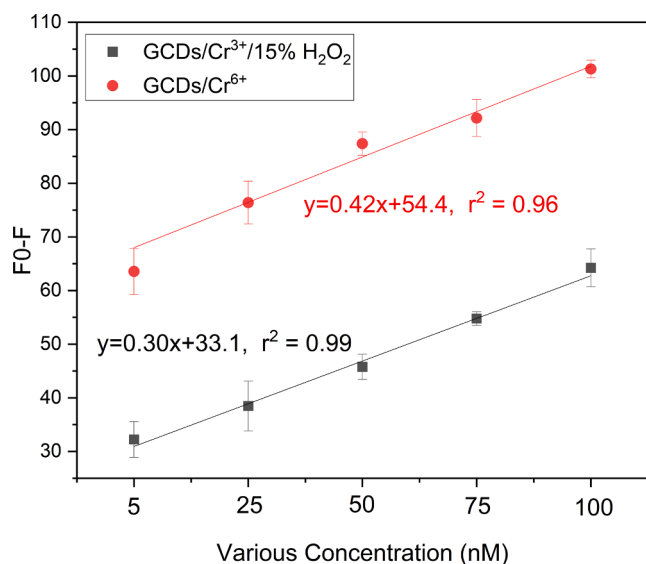


Fig. 11. Linear calibration plots of $F_0 - F$ versus various concentrations (5–100 nM) of (a) Cr^{6+} (a) and (b) Cr^{3+} plus H_2O_2 .

the fluorescence intensity of the blank and F represents the fluorescence intensity with varying concentrations of the metal ion. The experiments were involved conducting a quenching test at low concentrations at nanoscale: 5, 25, 50, 75, and 100 nM of Cr^{6+} (with a regression line of $y = 0.42x + 54.4$ and an r^2 value of 0.96) and Cr^{3+} plus H_2O_2 (with a regression line of $y = 0.30x + 33.1$ and an r^2 value of 0.99) as shown in Fig. 11. These results indicate a strong correlation and accurate detection of the concentration of Cr^{6+} ions. The findings of this study suggest that the CDs@GQDs nanohybrid composite possess the potential to serve as a novel sensor with exceptional selectivity and sensitivity in the determination of Cr^{6+} .

3.9.2. LOD and LOQ

The general statistical concept used to calculate the limit of detection (LOD) and limit of quantification (LOQ) were as follows: $\text{LOD} = 3\text{SD}/S$ and $\text{LOQ} = 10\text{SD}/S$. In these calculations, SD represents the standard deviation of three times the blank readings, and S represents the slope of the linear regression plot. The compilation of LOD and LOQ calculations are given in Table 3. The findings derived from both two linear curves for the detection of Cr^{6+} are as follows: the detection concentration range spans from 5 to 100 nM, with a limit of detection (LOD) of 15.76 nM and a limit of quantification (LOQ) of 47.76 nM. Similarly, the utilization of Cr^{3+} plus H_2O_2 also enables the detection of a concentration range from 5 to 100 nM, with LOD of 7.59 nM and LOQ of 23.01 nM. From this finding, total contents of Cr ions can be obtained from those data summation as mentioned above (Pimsin et al., 2022; Nugroho et al., 2023).

3.10. Application model for water sample analysis

The fluorescence quenching sensor was utilized to measure the concentration of chromium (VI) ions in some sample matrices, including drinking water and tap water, under the optimal conditions. The method accuracy was assessed by conducting a recovery study on the real water samples. The samples were augmented with three concentration ranges

Table 3

LOD and LOQ for Cr^{6+} detection of the developed method.

Linear curve	Regression equation	R^2	LOD (nM)	LOQ (nM)
Cr^{6+}	$y = 0.42x + 54.4$	0.96	15.76	47.76
Cr^{3+} plus H_2O_2	$y = 0.30x + 33.1$	0.99	7.59	23.01

(25, 50, and 100 nM) of the Cr^{6+} standard solution. Next, the relative percentage recoveries were determined using the formula: % recovery = $[C_{\text{found}} / C_{\text{added}}] \times 100$, where, C_{found} represents the concentration of the analyte after adding a known amount of standard to the real sample and C_{added} represents the concentration of the known amount of standard that was added to the real sample. The results of this calculation are presented in Table 4 and it's shown that the % recovery of drinking water that has been collected (sample 1 until 3) after spike Cr^{6+} in the range (0 – 75 nM) is around 89.3 – 110 %, and for the ta water (sample 1 and 2) in range 98.02 % – 114.23 %, The variation in numerical values observed in the %recovery, accompanied by the occurrence of an amount spike of sample Cr^{6+} , may be attributed to the potential influence of other minerals that can impact the operational efficacy of CDs@GQDs.

4. Conclusion

This study aimed to employ the one-pot pyrolysis method to produce graphene quantum dots (GQDs) from solid citric acid in the presence of hydrothermally derived carbon dots (CDs) obtained from the *Houttuynia cordata* plant extract to become the so-called novel CDs@GQDs nanohybrid composite. The CDs@GQDs were subjected to several characterization and morphology image techniques including X-ray photoelectron spectroscopy (XPS), transmission electron microscopy (TEM), field emission scanning electron microscopy with energy-dispersive X-ray spectroscopy (FE-SEM/EDX), Fourier-transform infrared spectroscopy (FT-IR), fluorescence spectroscopy, and UV-Visible absorption spectroscopy. Their quantum yield (15 %) was also determined. The CDs@GQDs demonstrate a significant level of fluorescence intensity, reaching its peak wavelength at 450 nm, when subjected to excitation at 355 nm. The optimization parameters affecting the detection of ultra-trace analysis of Cr^{6+} were investigated in details, including the effects of solution pH, concentration of EDTA as masking agent, ionic strength, reaction time including temperature, and oxidation of Cr^{3+} with 15 % H_2O_2 . The analytical properties of the developed approach were effectively validated. Consequently, the recovery study involving the spiked Cr^{6+} solution into real samples (drinking water and

Table 4

The Cr^{6+} contents found ($X \pm \text{SD}$, $n = 5$) and its recoveries of the spiked water samples.

Sample	Cr^{6+} added (nM)	Concentration found ($\pm \text{SD}$, $n = 5$)	% Recovery
Drinking water 1	0	–	–
	25	22.46 ± 2.98	89.85
	50	53.42 ± 3.45	106.85
	75	66.99 ± 3.17	89.32
Drinking water 2	0	–	–
	25	27.56 ± 3.98	110.24
	50	54.11 ± 4.65	108.23
	75	72.65 ± 3.16	96.86
Drinking water 3	0	–	–
	25	25.86 ± 1.06	103.44
	50	51.43 ± 4.37	102.86
	75	77.83 ± 2.73	103.77
Tap water 1	0	–	–
	25	24.51 ± 1.46	98.02
	50	53.88 ± 2.31	107.76
	75	83.30 ± 1.11	111.06
Tap water 2	0	–	–
	25	26.66 ± 3.07	106.63
	50	57.11 ± 3.11	114.23
	75	82.92 ± 2.16	110.56

tap water), yielded the results with satisfied accuracy and reproducibility. Consequently, the successful application of the CDs@GQDs nanohybrid composite as a green chelating sensor has enabled the selective measurement of trace amounts of Cr⁶⁺ in real water samples, hence enhancing its sensitivity in nanoscale level.

Declaration of competing interest

The authors declare that they have no known competing financial interests or personal relationships that could have appeared to influence the work reported in this paper.

Acknowledgements

The authors thank Materials Chemistry Research Center (MCRC), Department of Chemistry, Faculty of Science, and Center of Excellence for Innovation in Chemistry (PERCH-CIC), Khon Kaen University Consortium, Khon Kaen, Thailand for financial support.

References

- Abbasi, S., Bahiraei, A., 2012. Ultra trace quantification of chromium(VI) in food and water samples by highly sensitive catalytic adsorptive stripping voltammetry with rubeanic acid. *Food Chem.* 133, 1075–1080.
- Ahn, J., Chae, H.S., Chin, Y.W., Kim, J., 2017. Alkaloids from Aerial parts of *houltuynia cordata* and their anti-inflammatory activity. *Bioorganic Med. Chem. Lett.* 27, 2807–2811.
- Almaguer-Busso, G., Velasco-Martínez, G., Carreno-Aguilera, G., Gutiérrez-Granados, S., Torres-Reyes, E., Alatorre-Ordaz, A., 2009. A comparative study of global hexavalent chromium removal by chemical and electrochemical processes. *Electrochem. Commun.* 11, 1097–1100.
- Anderson, R., Polansky, M., Bryden, N., Patterson, K., Veillon, C., Glinsmann, W., 1983. Effects of chromium supplementation on urinary Cr excretion of human subjects and correlation of Cr excretion with selected clinical parameters. *J. Nutr.* 113, 276.
- Aumber, A., Tanveer, A.T., Steve, J.B., Tuti, M.L., Anh, N.P., 2020. High yield synthesis of graphene quantum dots from biomass waste as a highly selective probe for Fe³⁺ sensing. *Sci Rep.* 10, 21262.
- Bu, L., Peng, J., Peng, H., Liu, S., Xiao, H., Liu, D., Pan, Z., Chen, Y., Chen, F., He, Y., 2016. Fluorescent carbon dots for the sensitive detection of Cr(VI) in aqueous media and their application in test papers. *RSC Advances* 6, 95469–95475.
- Chaabane, M., Elweji, A., Ghorbel, B., Boudawara, T., Zeghal, N., Soudani, N., Citrus aurantium, L. 2017. Peel extract mitigates hexavalent chromium-induced oxidative stress and cardiotoxicity in adult rats. *Pharmaceutical and Biomedical Research.* 3, 8–18.
- Chang, J.S., Chiang, L.C., Chen, C.C., Liu, L.T., Wang, K.C., Lin, C.C., 2001. Atileukemic activity of *bidenspilosa* L. Var. minor (Blume) sherff and *houltuynia cordata* thunb. *Am. J. Chin. Med.* 29, 303–312.
- Chen, Q.Y., Murphy, A., Sun, H., Costa, M., 2019. Molecular and epigenetic mechanisms of Cr(VI)-induced carcinogenesis. *Toxicol. Appl. Pharmacol.* 377, 114636.
- Chiang, L.C., Chang, J.S., Chen, C.C., Ng, L.T., Lin, C.C., 2003. Anti-Herpes Simplex Virus Activity of *Bidens Pilosa* and *Houltuynia Cordata*. *Am. J. Chin. Med.* 31, 355–362.
- Chou, S.C., Su, C.R., Ku, Y.C., Wu, T.S., 2009. The constituents and their bioactivities of *houltuynia cordata*. *Chem. Pharm. Bull.* 57, 1227–1230.
- Cieslak, W., Pap, K., Bunch, D., Reineks, E., Jackson, R., Steinle, R., Wang, S., 2013. Highly sensitive measurement of whole blood chromium by inductively coupled plasma mass spectrometry. *Clin. Biochem.* 46, 266–270.
- Dayan, A., Paine, A., 2001. Mechanisms of chromium toxicity, carcinogenicity and allergenicity: Review of the literature from 1985 to 2000. *Hum. Exp. Toxicol.* 20, 439.
- Fletcher, A.N., 1969. Quinine sulfate as a fluorescence quantum yield standard. *J. Photochem. Photobiol.* 439–444.
- Gao, Z.H., Lin, Z.Z., Chen, X.M., Lai, Z.Z., Huang, Z.Y., 2016. A fluorescent probe based on N-doped carbon dots for highly sensitive detection of Hg²⁺ in aqueous solutions. *Anal. Methods.* 222, 965–971.
- Gontrani, L., Bauer, E.M., Nucara, A., Tagliatesta, P., Carbone, M., 2022. Highly specific silver ion detection by fluorescent carbon quantum dots. *Chemosensors* 10, 362.
- Guo, Y.M., Wang, Z., Shao, H.W., Jiang, X., 2013. Hydrothermal synthesis of highly fluorescent carbon nanoparticles from sodium citrate and their use for the detection of mercury ions. *Carbon.* 52, 583–589.
- Haider, G., Roy, P., Chiang, C.W., Tan, W.C., Liou, Y.R., Chang, H.T., Liang, C.T., Shih, W.H., Chen, Y.F., 2016. Electrical-polarization-induced ultrahigh responsivity photodetectors based on graphene and graphene quantum dots. *Adv. Funct. Mater.* 4, 620–628.
- Himeno, S., Nakashima, Y., Sano, K.-I., 1998. Simultaneous determination of chromium (VI) and chromium(III) by capillary electrophoresis. *Anal. Sci.* 14, 369–373.
- Hossain, M.A., Kumita, M., Michigami, Y., Islam, T.S., Mori, S., 2005. Rapid speciation analysis of Cr(VI) and Cr(III) by reversed-phase high-performance liquid chromatography with UV detection. *J. Chromatogr. Sci.* 43, 98–103.
- Iztleuov, M., Kaliev, A., Turganbaeva, A., Yesmukhanova, D., Akhmetova, A., Temirbayeva, A., Yerbolat, I., Gulmira, I., 2020. The effect of sodium tetraborate on chromium-induced oxidative damages in rats lung tissue. *Biomed. Pharmacol. J.* 13.
- Kart, A., Koc, E., Dalginli, K.Y., Gulmez, C., Sertcelik, M., Atakisi, O., 2016. The therapeutic role of glutathione in oxidative stress and oxidative DNA damage caused by hexavalent chromium. *Biol. Trace Elem. Res.* 174, 387–391.
- Lei, Y., Wu, Y., Jiang, Z., Ouyang, Z., Hu, J., Lin, Y., Du, P., Zou, B., 2021. Effect of various mass ratios of graphene quantum dots doping on the photoelectric performance of ZnSe-GQDs nanocomposites. *Mater. Sci. Semicond. Process.* 128, 105740.
- Li, J., Rehman, M.U., Zhang, H., Iqbal, M.K., Mehmood, K., Huang, S., Nabi, F., 2017. Sciences, A. antibacterial effect of the water extract of *houltuynia cordata* water extract against multi-drug resistant. *Southeast Asian J. Trop. Med. Public Health* 48, 1260–1266.
- Lim, S.Y., Shen, W., Gao, Z., 2015. Carbon quantum dots and their applications. *Chem. Soc. Rev.* 44, 362–381.
- Lu, H.M., Liang, Y.Z., Yi, L.Z., Wu, X.J., 2006. Anti-Inflammatory Effect of *Houltuynia Cordata* Injection. *J. Ethnopharmacol.* 104, 245–249.
- Ma, Q., Wei, R., Wang, Z., Liu, W., Sang, Z., Li, Y., Huang, H., 2017. Bioactive alkaloids from the aerial parts of *houltuynia cordata*. *J. Ethnopharmacol.* 195, 166–172.
- Machle, W., Gregorius, F., 1948. Cancer of the respiratory system in the United States chromate-producing industry. *Public Health Rep.* 63, 1114–1127.
- Manjunatha, K.B., Bhat, R.S., Shashidhara, A., et al., 2021. Antimicrobial and nonlinear optical studies of copper oxide nanoparticles. *J. Electron. Mater.* 50, 3415–3421.
- Manjunatha, K.B., Bhat, R.S., Raviprabha, K., et al., 2023. Synthesis, structural features, and optical limiting application of silicon carbide nanoflakes. *J. Mater. Sci: Mater. Electron.* 34, 1885.
- Morozan, A., Jaouen, F., 2012. Metal organic frameworks for electrochemical applications. *Energy Environ. Sci.* 5, 9269–9290.
- Nugroho, D., Oh, W.-C., Chanthai, S., Benchawattananon, 2022. R. improving minutiae image of latent fingerprint detection on non-porous surface materials under UV light using sulfur doped carbon quantum dots from *magnolia grandiflora* flower. *Nanomaterials.* 12, 3277.
- Nugroho, D., Keawprom, C., Chanthai, S., Oh, W.-C., Benchawattananon, R., 2022. Highly sensitive fingerprint detection under UV light on non porous surface using starch-powder based luminol-doped carbon dots (N-CDs) from tender coconut water as a green carbon source. *Nanomaterials* 12, 400.
- Nugroho, D., Chanthai, S., Oh, W.-C., Benchawattananon, R., 2023. Fluorophores-rich natural powder from selected medicinal plants for detection latent fingerprints and cyanide. *Science Progress* 106, 1.
- Onchoke, K.K., Sasu, S.A., 2016. Determination of Hexavalent Chromium (Cr(VI)) Concentrations via Ion Chromatography and UV-vis Spectrophotometry in Samples Collected from Nacogdoches Wastewater Treatment Plant, East Texas (USA). *Adv. Environ. Chem.* 10.
- Onchoke, K.K., Sasu, S.A., 2016. Determination of hexavalent chromium (Cr(VI)) concentrations via ion chromatography and UV-Vis spectrophotometry in samples collected from nacogdoches wastewater treatment plant, East Texas (USA). *Advances in Environmental Chemistry* 1–10.
- Park, E., Kum, S., Wang, C., Park, S.Y., Kim, B.S., Schuller-Levis, G., 2005. Anti-inflammatory activity of herbal medicines: Inhibition of nitric oxide production and tumor necrosis factor- α secretion in an activated macrophage-like cell line. *Am. J. Chin. Med.* 33, 415–424.
- Pimsin, N., Keawprom, C., Areeerob, Y., et al., 2022. Selective Fe(II)-fluorescence sensor with validated two-consecutive working range using N, S, I-GQDs associated with garlic extract as an auxiliary green chelating agent, *RSC. Advances* 12, 14356–14367.
- Posthuma-Trumpie, G.A., Wichers, J.H., Koets, M., Berendsen, L.B.J.M., Amerongen, A. V., 2012. Amorphous carbon nanoparticles: a versatile label for rapid diagnostic (immuno)assays. *Anal. Bioanal. Chem.* 402, 593–600.
- Rahman, H., Hoque, N., Sarker, P.K., Safa, A., 2020. Assessment of hexavalent chromium pollution in Buriganga and Dhaleshwari river water bodies adjacent to Tannery Estates in Bangladesh. *MIST Int J Sci Technol* 8, 11–15.
- Shobana, N., Aruldas, M.M., Tothhawng, L., Loganathan, A., Balaji, S., Kumar, M.K., Banu, L.A.S., Navin, A.K., Mayilvanan, C., Ilangovan, R., 2017. Transient gestational exposure to drinking water containing excess hexavalent chromium modifies insulin signaling in liver and skeletal muscle of rat progeny. *Chem. Biol. Interact.* 277, 119–128.
- Sokoll, R., Gesek, M., Ras-Norynska, M., Michalczuk, M., Koziatek, S., 2015. Biochemical parameters in Japanese quails *Coturnix coturnix japonica* infected with coccidia and treated with Toltrazuril. *Pol. J. Vet. Sci.* 18, 79.
- Suchana, S.A., Ahmed, M.S., Islam, S.M., Rahman, M.L., Rohani, M.F., Ferdusi, T., Ahmmad, A.S., Fatema, M.K., Badruzzaman, M., Shahjahan, M., 2020. Chromium exposure causes structural aberrations of erythrocytes, gills, liver, kidney, and genetic damage in striped catfish pangasianodon hypophthalmus. *Biol. Trace Elem. Res.* 1–17.
- Tao, H.Q., Yang, K., Ma, Z., Wan, J.M., Zhang, Y.J., Kang, Z.H., Liu, Z., 2012. In vivo NIR fluorescence imaging, biodistribution, and toxicology of photoluminescent carbon dots produced from carbon nanotubes and graphite. *Small Journ.* 8, 281–290.
- Tariq, A.A., Mohamed, I.M., Gaber, M.A.M., Mohammed, A., Mahmoud, M.H.H., Tushar, K., Ahmed, S., El-Bindary, M.A., 2021. Mesopores silica nanotubes-based sensors for the highly selective and rapid detection of Fe²⁺ ions in wastewater, boiler system units and biological samples. *Anal. Chim. Acta.* 1180, 331180.
- Tetsuka, H., Nagoya, A., Tamura, S.I., 2016. Graphene/nitrogen - functionalized graphene quantum dot hybrid broadband photodetectors with a buffer layer of boron nitride nanosheets. *Nanoscale.* 47, 19677–19683.

- Varun, A.C., Rajnish, K., Naveen, K., Akash, D., Changanamkandath, R., Kim, K.H., 2018. Synthesis and spectroscopic studies of functionalized graphene quantum dots with diverse fluorescence characteristics. *RSC Adv.* 8, 11446–11454.
- Vassileva, E., Hadjiivanov, K., Stoychev, T., Daiev, C., 2000. Chromium speciation analysis by solid-phase extraction on a high surface area TiO₂. *Anst.* 125, 693–698.
- Wang, Y., Anilkumar, P., Cao, L., Liu, J.H., Luo, P.G., Tackett, K.N., Sahu, S., Wang, P., Wang, X., Sun, Y.P., 2011. Carbon dots of different composition and surface functionalization: cytotoxicity issues relevant to fluorescence cell imaging. *Exp. Biol. Med.* 236, 1231–1238.
- Wang, H., Liu, S., Xie, Y., Bi, J., Li, Y., Song, Y., Tan, M., 2018. Facile one-step synthesis of highly luminescent N-doped carbon dots as an efficient fluorescent probe for chromium(vi) detection based on the inner filter effect. *Ne J Chem.* 42 (5), 3729–3735.
- Zhan, M., Yu, H., Li, L., Ngu, D., 2019. Detection of hexavalent chromium by copper sulfide nanocomposites. *Anal. Chem.* 91, 2058–2065.